Effects of Phosphorus Addition on Selectivity and Stability of Pd Model Catalysts during Cyclohexene Dehydrogenation

Abinaya Sampath, and David W. Flaherty*

Supporting Information

Department of Chemical and Biomolecular Engineering
University of Illinois Urbana-Champaign, Urbana, IL 61801

*Corresponding Author

Phone: (217) 244-2816

Email: dwflhrty@illinois.edu

Section S1. Low Energy Electron Diffraction Patterns of P_x-Pd Surfaces

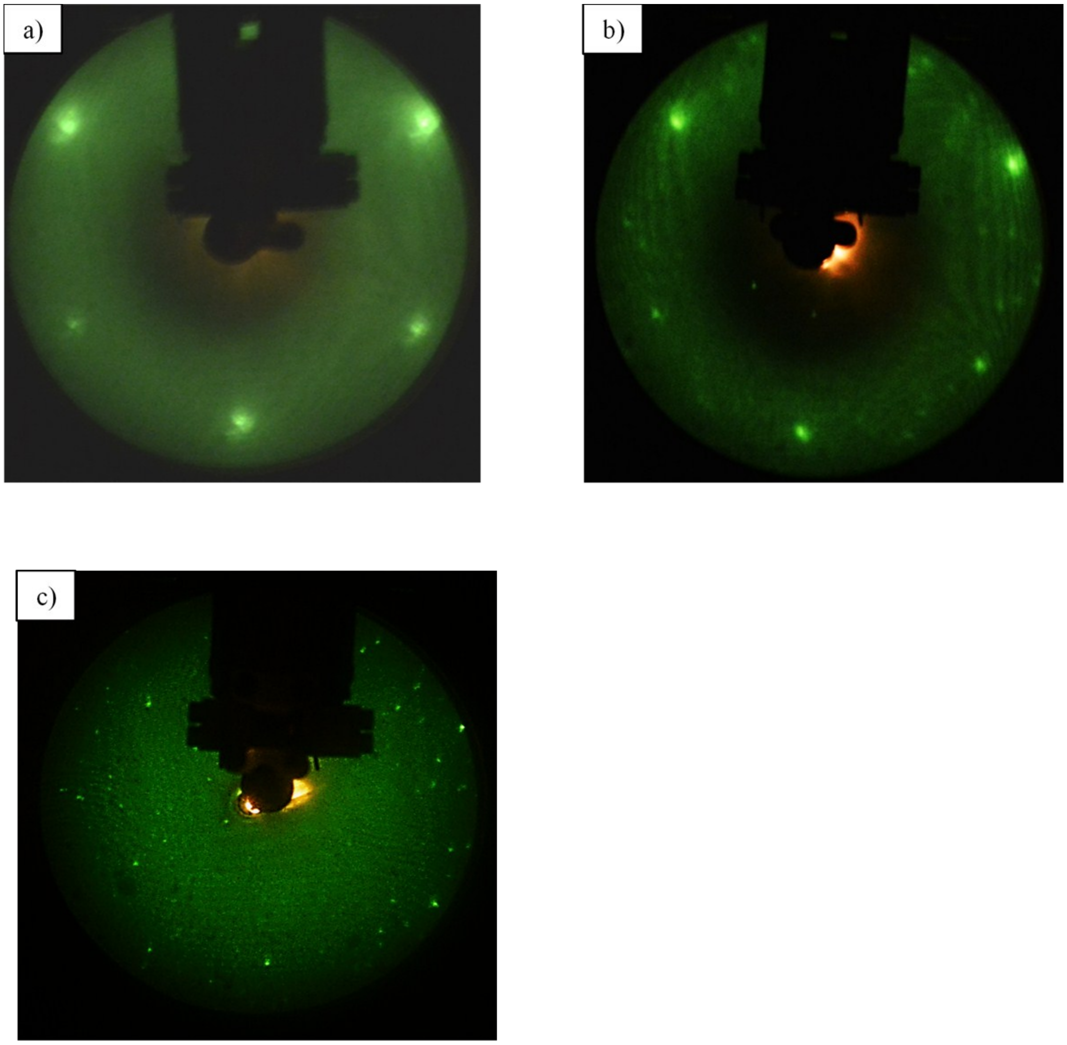

Figure S1. Low-energy electron diffraction pattern of a) Pd(111) with a (1x1) pattern at a beam voltage of 40 eV. b) $P_{0.17}$-Pd at a beam voltage of 40 eV and c) $P_{0.34}$-Pd at a beam voltage of 45 eV.

Section 2. Desorption Profiles of C_6H_{10} during TPR of C_6H_{10} over P_x-Pd Surfaces

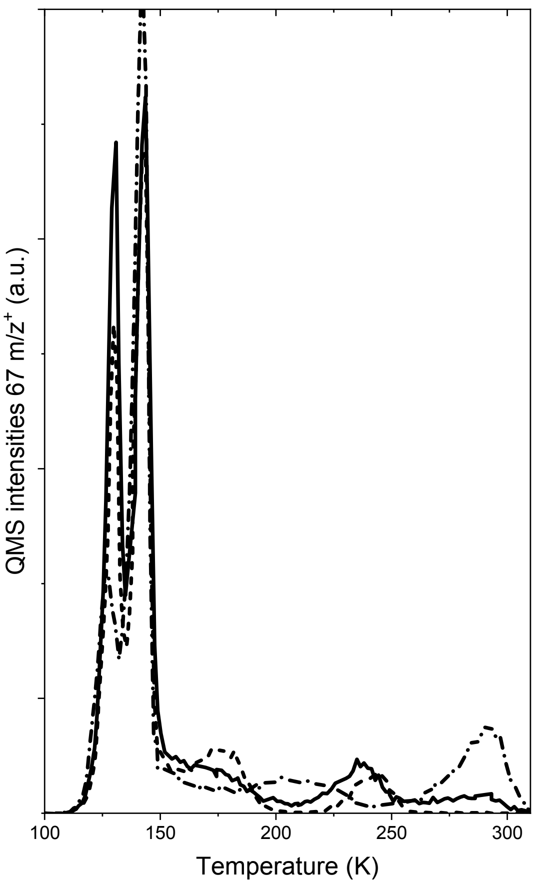

Figure S2. Desorption profile of C_6H_{10} (67 m/z$^+$) from TPR of 0.4 ML C_6H_{10} adsorbed at 77 K on Pd (dashed), 0.4 ML of C_6H_{10} adsorbed at 77 K on $P_{0.17}$-Pd (solid), and 0.3 ML C_6H_{10} adsorbed at 77 K on $P_{0.34}$-Pd (dash dot) and heated at 3 K s^{-1}.

Section S3. Desorption Profiles of C_6H_6 and H_2 on P_x-Pd Surfaces

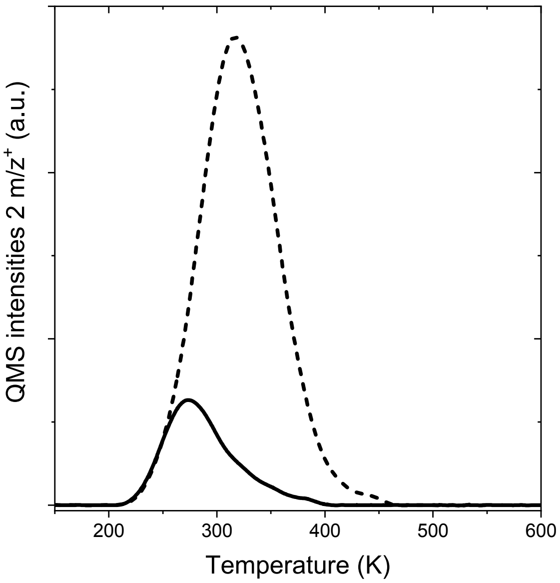

Figure S3. Desorption profiles of H_2 from TPD of saturation coverages of H_2 adsorbed at 77 K and heated at 3 K s^{-1} on Pd (dashed) and $P_{0.34}$-Pd (solid).

Figure S3 shows the desorption profiles of H_2 from the recombination of chemisorbed atomic hydrogen on Pd[1] and $P_{0.34}$-Pd surfaces, and we see that the peak desorption temperature decreases about 45 K on $P_{0.34}$-Pd (270 K) when compared to Pd (315 K). This is in line with the observation of decreased binding energy of H_2 in the presence of P over $Ni_2P(0001)$ when compared to Ni(111) which could be due to electronic differences in the presence of P and the creation of P-modified binding sites.[2]

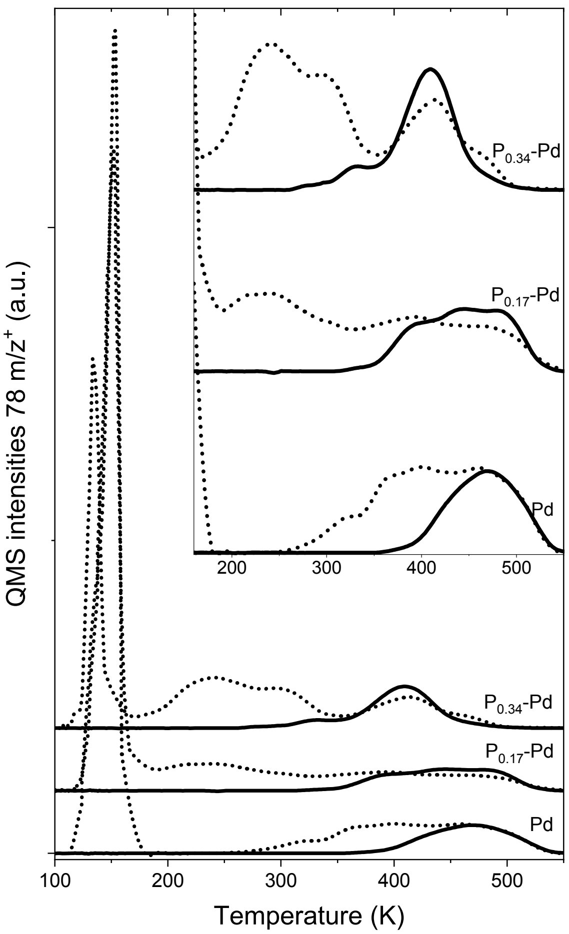

Figure S4. Desorption profiles of C_6H_6 from TPR of C_6H_6 (dashed) and C_6H_{10} (solid) adsorbed at 77 K on Pd, $P_{0.17}$-Pd, $P_{0.34}$-Pd and heated at 3 K s^{-1}.

Figure S4 shows the desorption profiles of C_6H_6 from TPR of C_6H_{10} and C_6H_6. The overlap of the desorption peaks of molecular desorption of C_6H_6 and C_6H_6 formed from C_6H_{10} dehydrogenation demonstrates that the desorption of C_6H_6 is the kinetically relevant step of the formation of C_6H_6 from C_6H_{10}. Based on the highest peak desorption temperatures of C_6H_6, assuming a prefactor of 10^{13} s^{-1}, using first order Redhead analysis, C_6H_6 binds about 14 kJ mol^{-1} more weakly on $P_{0.34}$-Pd (106 kJ mol^{-1}) than on Pd (120 kJ mol^{-1}).

Section S4. King and Wells Measurements[3] for C_6H_{10} Dehydrogenation Selectivity Calculations

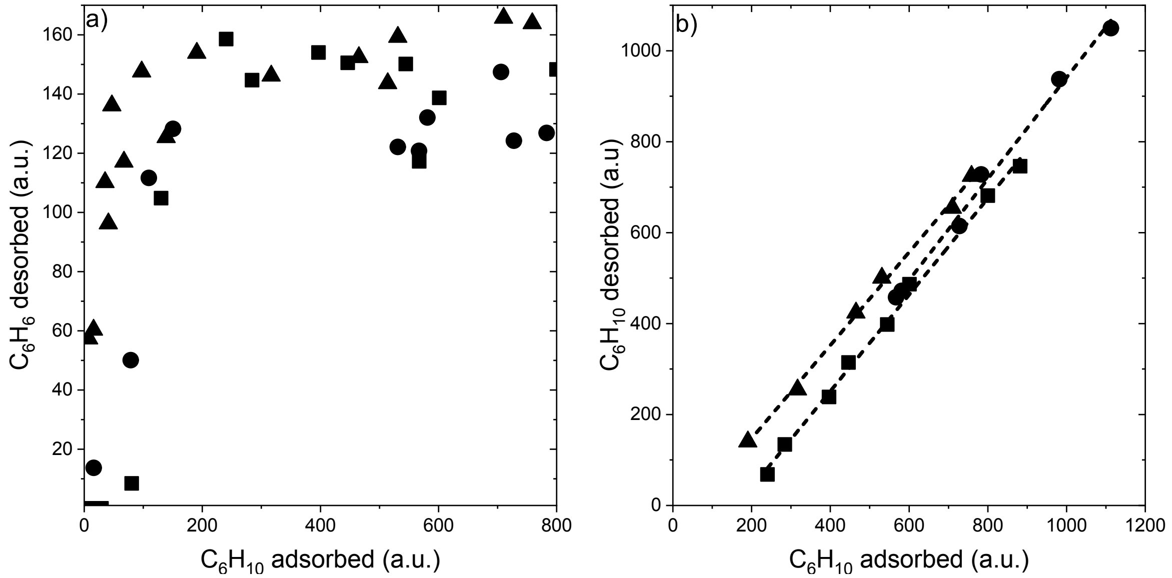

Figure S5. a) Total C_6H_6 desorbed and total C_6H_{10} adsorbed during the TPR of different initial coverages of C_6H_{10} adsorbed at 77 K on Pd (■), $P_{0.17}$-Pd (●), and $Pd_{0.34}$-Pd (▲) and heated at 3 K s^{-1} b) Total C_6H_{10} desorbed as a function of total C_6H_{10} adsorbed during the TPR of 0.14 ML or higher coverage of C_6H_{10} adsorbed on Pd (■), $P_{0.17}$-Pd (●), and $Pd_{0.34}$-Pd (▲) at 77 K and heated at 3 K s^{-1}.

During the TPR of C_6H_{10}, the formation of C_6H_6 is constant for C_6H_{10} surface coverages (obtained from **Figure S5a**) greater than 0.14 ML[4-5] which is assumed to the saturation coverage of C_6H_{10} on Pd(111). The amount of C_6H_{10} adsorbed is measured using King and Wells measurements and the amount of C_6H_{10} desorbed and C_6H_6 formed are calculated by integrating the desorption profiles from the TPR of C_6H_{10}. In the C_6H_{10} surface coverage range of constant C_6H_6 desorption, the intercept of the graph of C_6H_{10} desorbed versus C_6H_{10} adsorbed is the measure of C_6H_{10} consumed during the TPR of C_6H_{10} that either dehydrogenates to form C_6H_6 or decomposes to coke on the surface.

Section S5. Rate Expression Derivation for C_6H_{10} Dehydrogenation on Pd and P_x-Pd Surfaces

Scheme S1: Proposed sequence of steps for C_6H_{10} dehydrogenation on P_x-Pd catalysts. Note: * denotes unoccupied catalytic site; X and X* represent a gas-phase species and the corresponding bound surface intermediate, respectively; $\xrightarrow{\wedge}$ indicates that the elementary step is kinetically relevant; $\overset{\longrightarrow}{\longrightarrow}$ indicates a series of steps that form carbon deposits on the catalyst surface; k_a represents the rate constant for the elementary step (5.a); x and y represent a whole number from 1 to 5.

$$
\begin{array}{llllll}
C_6H_{10} & + * & \xrightarrow{k_1} & C_6H_{10}* & & (5.1) \\
C_6H_{10}* & + * & \xrightarrow{k_2} & C_6H_9* & + H* & (5.2) \\
C_6H_9* & + * & \xrightarrow{k_3} & C_6H_8* & + H* & (5.3) \\
C_6H_8* & + * & \xrightarrow{k_4} & C_6H_7* & + H* & (5.4) \\
C_6H_7* & + * & \xrightarrow{k_5} & C_6H_6* & + H* & (5.5) \\
C_6H_6* & & \overset{k_6}{\xrightarrow{\wedge}} & C_6H_6 & + * & (5.6) \\
2H* & & \xrightarrow{k_7} & H_2 & + 2* & (5.7) \\
C_6H_6* & + * & \overset{k_8}{\overset{\longrightarrow}{\longrightarrow}} & C_xH_y* & + C_{(6-x)}H_{(6-y)}* & (5.8)
\end{array}
$$

$$r_1 = k_1[C_6H_{10}][*] \qquad \text{(S5.1)}$$

$$r_6 = k_6[C_6H_6*] \qquad \text{(S5.2)}$$

$$r_8 = k_8[C_6H_6*][\frac{*}{L}] \qquad \text{(S5.3)}$$

$$\text{(S5.4)} \qquad [L] = [C_6H_{10}*] + [C_6H_9*] + [C_6H_8*] + [C_6H_7*] + [C_6H_6*] + [H*] + [*]$$

The rate of elementary steps (5.1), (5.6), and (5.8) are given by **Equation S5.1, S5.2, and S5.3**, respectively. Here, [L] represents the number of active sites defined by **Equation S5.4**, excluding the active sites poisoned by the irreversible formation of coke. [C_6H_{10}*], [C_6 H_9*], [C_6 H_8*], [C_6 H_7*], [C_6H_6*], [H*], [*] represent the surface coverages of the surface-bound intermediates C_6H_{10}*, C_6H_9*, C_6H_8*, C_6H_7*, C_6H_6*, H*, and unoccupied catalytic sites respectively. We assume that all the elementary steps are catalyzed by the same type of catalytic sites. Applying pseudo-steady state assumptions (PSSA) on the intermediates C_6H_{10}*, C_6H_9*, C_6 H_8*, C_6H_7*, C_6H_6*, we arrive at the **Equation S5.5** which implies that the rate of C_6H_{10} adsorption equals the rate of C_6H_6 desorption and overall coking of the surface. Using **Equation S5.5**, the surface coverage of C_6H_6*is given by **Equation 5.6**. Substituting for surface coverage of C_6H_6* in **Equation S5.2**, we derive the rate of C_6H_6 formation in **Equation S5.7.** The reactants and products (i.e., C_6H_{10}, H_2, C_6H_6) desorb completely from these surfaces at temperatures below 550 K as discussed in the main text, which suggests that catalytically active sites are predominantly bare during steady-state catalysis at 525 – 650 K (i.e., unoccupied sites are the most abundant reactive intermediate, MARI). C_6H_6

desorption is the kinetically relevant step on Pd and P-modified surfaces for the formation of C_6H_6 from C_6H_{10} dehydrogenation as discussed in **Section S3**. Following substitution for empty sites to be the MARI in the rate of kinetically relevant C_6H_6 desorption, the rate of C_6H_6 formation is represented in **Equation S5.8**.

$$r_1 = r_6 + r_8 \qquad \text{(S5.5)}$$

$$[C_6H_6*] = \frac{k_1[C_6H_{10}][*]}{\left(k_6 + k_8[\frac{*}{L}]\right)} \qquad \text{(S5.6)}$$

$$r_6 = \frac{k_6k_1[C_6H_{10}][*]}{\left(k_6 + k_8[\frac{*}{L}]\right)} \qquad \text{(S5.7)}$$

$$\frac{r}{[L]} = \frac{k_6k_1[C_6H_{10}]}{k_6 + k_8} \qquad \text{(S5.8)}$$

Here, we observe that the rate of C_6H_6 formation is proportional to the near surface concentration of C_6H_{10} by applying PSSA on the dehydrogenated intermediates and assuming the desorption of C_6H_6 to be kinetically relevant. However, assuming any other step (5.1) through (5.5) to be kinetically relevant and applying PSSA on the dehydrogenated intermediates would result in a similar rate expression for C_6H_6, which is proportional to the concentration of C_6H_{10} as long as the empty sites are the MARI.

Section S6. Modeling of Rate of Deactivation of P_x-Pd Surfaces

There is an exponential decay in the rate of formation of C_6H_6 with time and this decay results from the loss in the number of active sites for C_6H_{10} dehydrogenation due to the formation of coke. Hence, the decay can be modeled by accounting for the loss in the number of active sites. The decay in the rate can be modeled as an exponential decay resulting from coking due to C_6H_6 derived intermediates that is proportional to the surface coverage of C_6H_6.[6-7] Given k_1, k_6, k_8, and $[C_6H_{10}]$ remain constant, the decay results from the decrease in the number of active sites from coking due to decomposition of C_6H_6 (**Equation S5.3**). Substituting for the surface coverage of C_6H_6 from **Equation S5.6**, we obtain **Equation S6.1**. However, there is also active dissolution of the coke into the bulk of the sample which is proportional to the total number of catalytic sites poisoned by the formation of coke, $[L]_c$, given by **Equation S6.2** where $[L]_0$ is the total number of catalytic sites on the pristine catalyst surface and $[L]$ is the total number of catalytically active sites at any given time. The rate of dissolution of coke can be written as r_d proportional to the poisoned sites (**Equation S6.3**), where k_{diss} is the rate constant. Hence, the rate of decrease of the catalytically active sites equals the difference of rate of formation of poisoned sites and the rate of coke dissolution, which is given by **Equation S6.4**. Substituting for r_8, r_d gives the **Equation S6.5.** Assuming empty catalytic sites to be the MARI, the empty catalytic sites can be approximated to be the total number of active sites and the rate of coking is simplified to form in **Equation S6.6**.

$$r_8 = \frac{k_8 k_1 [C_6H_{10}][*]^2}{\left(k_6 + k_8[\frac{*}{L}]\right)[L]} \qquad \text{(S6.1)}$$

$$[L]_c = [L]_0 - [L] \qquad \text{(S6.2)}$$

$$r_d = k_{diss}([L]_0 - [L]) \qquad \text{(S6.3)}$$

$$-\frac{d[L]}{dt} = \frac{d[L]_c}{dt} = -r_d + r_8 \qquad \text{(S6.4)}$$

$$\frac{d[L]}{dt} = k_{diss}([L]_0 - [L]) - \frac{k_8 k_1 [C_6H_{10}][*]^2}{\left(k_6 + k_8\left[\frac{*}{L}\right]\right)[L]} \qquad \text{(S6.5)}$$

$$\frac{d[L]}{dt} = k_{diss}([L]_0 - [L]) - \frac{k_8 k_1 [C_6H_{10}][L]}{(k_6 + k_8)} \qquad \text{(S6.6)}$$

Solving the differential equation with the initial conditions as represented in **Equation S6.7**, the total number of active sites at any given time is represented by **Equation S6.8,** where k_d is the apparent deactivation constant. The apparent deactivation rate constant, k_d, in **Equation S6.8**, can be represented in terms of other rate constants in **Equation S6.9**. The rate of C_6H_6 formation, with accounting for the loss in the total number of active catalytic sites is given by **Equation S6.10**, where $[L]_\infty$ represents the total number of catalytically active sites at infinite time and is given by **Equation S6.11**.

$$[L] = [L]_0 \tag{S6.7}$$

$$[L] = ([L]_0 - \frac{k_{diss}[L]_0}{k_d})\exp^{-k_d t} + \frac{k_{diss}[L]_0}{k_d} \tag{S6.8}$$

$$k_d = \frac{k_8 k_1 [C_6H_{10}]}{(k_6 + k_8)} + k_{diss} \tag{S6.9}$$

$$r = \frac{k_6 k_1 [C_6H_{10}]}{k_6 + k_8}\left(([L]_0 - [L]_\infty)\exp\left(-k_d t\right)\right) + \frac{k_6 k_1 [C_6H_{10}][L]_\infty}{(k_6 + k_8)} \tag{S6.10}$$

$$[L]_\infty = \frac{k_{diss}[L]_0}{k_d} \tag{S6.11}$$

From **Equation S6.10**, we see that the rate of C_6H_6 formation is maximum at time t = 0, followed by a steady exponential decay in the rate resulting from the loss of active sites due to coke formation and reaches a steady-state at infinite time due to the balance in the number of active sites being coked and the active dissolution of the coke into the subsurface of the catalyst.

Section S7. Desorption Profiles of Products, Conversion, and Selectivities during RMBS of C_6H_{10} and C_6H_6

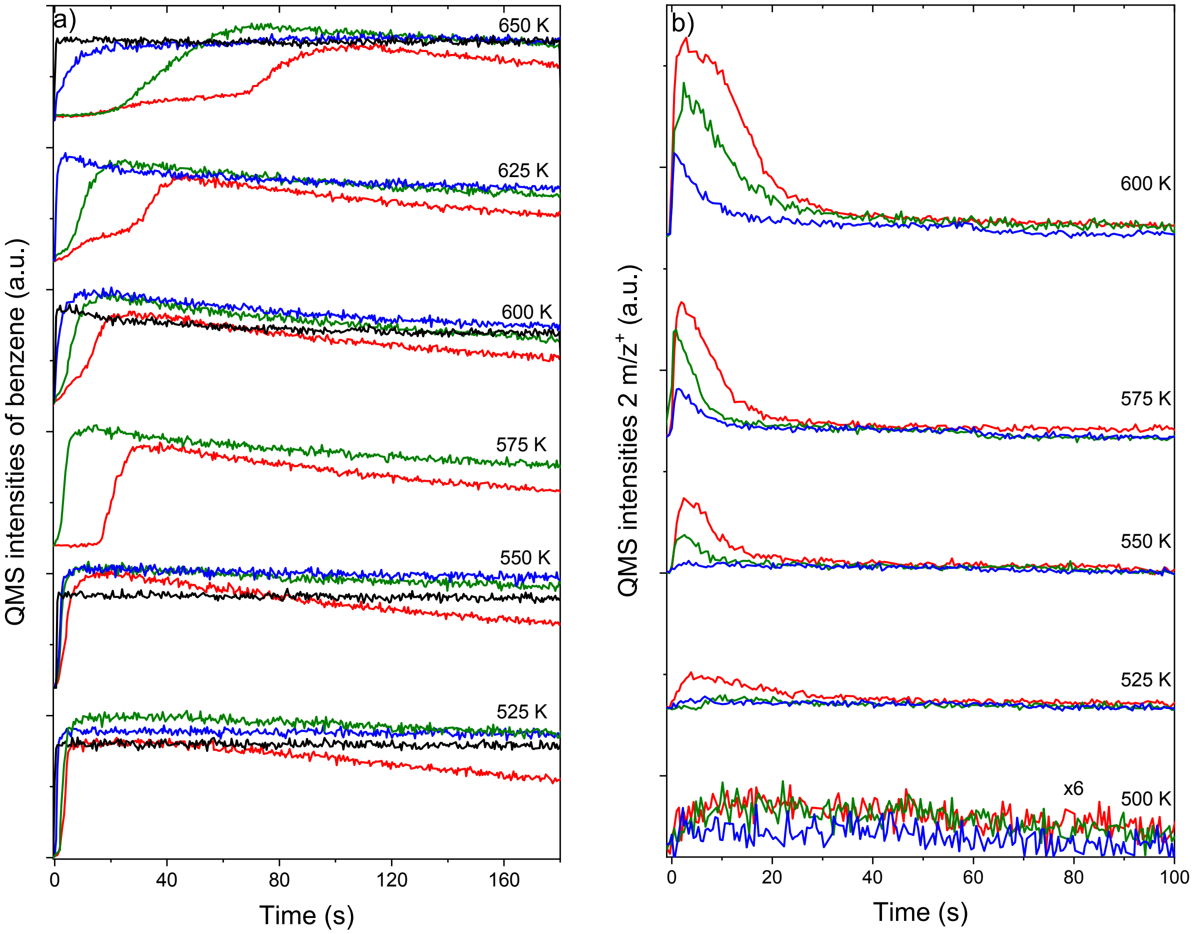

Figure S6. a) Rate of formation of C_6H_6 as a function of time during the RMBS of C_6H_{10} at different temperatures on Pd (red), $P_{0.17}$-Pd (green), $P_{0.25}$-Pd (blue), and $P_{0.34}$-Pd (black). b) Rate of formation of H_2 as a function of time during the RMBS of C_6H_6 at different temperatures on Pd (red), $P_{0.17}$-Pd (green), and $P_{0.25}$-Pd (blue).

Figure S6a shows the desorption of C_6H_6 formed from the C_6H_{10} dehydrogenation when the catalyst surface is impinged with the reactant beam at time t = 0. With increase in the amount of P on the catalyst surface, there is a decrease in the initial induction time for the formation of C_6H_6 which is due to the inhibition of the decomposition of C_6H_6 formed at lower coverages in the presence of P in the temperature range of 525 – 650 K. With increase in temperature, there is significant increase in the decomposition of the surface intermediates to coke as compared to the dehydrogenation to C_6H_6 as seen from the decrease in the amount of C_6H_6 formed over time. **Figure S6b** shows the formation of H_2 as a function of time when the catalyst surfaces are impinged with C_6H_6 at time t = 0. There is an instantaneous formation of H_2, which decreases with time due to the loss in the active sites from coke formation on these catalyst surfaces. At any given temperature in the range of 500 – 600 K, we observe that the amount of H_2 formed is significantly reduced with the increase in the amount of P on the surface. This corroborates the decrease in the C_6H_6 decomposition formed from C_6H_{10} in **Figure S6a**. Similar to an increase in the coke formation against C_6H_6 formation from RMBS of C_6H_{10} in **Figure S6a**, the rate of H_2 formation from the decomposition of C_6H_6 increases with temperature.

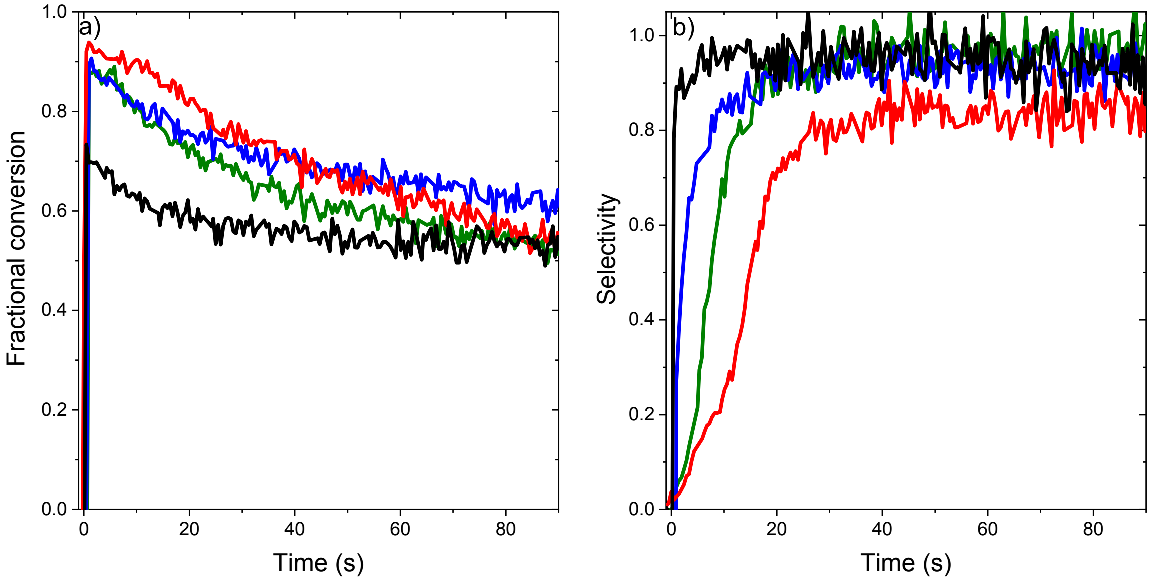

Figure S7. a) Fractional conversion of C_6H_{10} as a function of time during the RMBS of C_6H_{10} at 600 K over Pd (red), $P_{0.17}$-Pd (green), $P_{0.25}$-Pd (blue), and $P_{0.34}$-Pd (black). b) Selectivity of C_6H_6 as a function of time during the RMBS of C_6H_6 at 600 K over Pd (red), $P_{0.17}$-Pd (green), and $P_{0.25}$-Pd (blue), and $P_{0.34}$-Pd (black).

Figure S7 shows the conversion of C_6H_{10} and the selectivity of C_6H_6 as a function of time during RMBS of C_6H_{10} when the catalyst surface is impinged with C_6H_{10} at time t = 0 at 600 K. The initial conversion is ~90% over Pd, $P_{0.17}$-Pd, and $P_{0.25}$-Pd, whereas the conversion is ~70% over $P_{0.34}$-Pd. The lower conversion over $P_{0.34}$-Pd could be due to the loss in the number of active catalytic sites with higher amounts of P. C_6H_6 forms as soon as $P_{0.34}$-Pd is impinged with C_6H_{10} and almost a constant selectivity of ~95% is reached. This reflects in a gradual decrease in the conversion of C_6H_{10} over $P_{0.34}$-Pd due to the loss in the active catalytic sites. As the P content decreases ($P_{0.17}$-Pd and $P_{0.25}$-Pd surfaces), the initial amount of coking increases and there is an induction time for the selectivity to reach ~95%. Since the rate of coke formation leading to loss in active catalytic sites is larger with decrease in the amount of P on the surface, there is a more rapid decay of the catalyst surfaces when compared to $P_{0.34}$-Pd. This decay is further accentuated over Pd due to larger amount of coke formation on the surface.

References

1 G. E. Gdowski, T. E. Felter and R. H. Stulen, *Surf. Sci.,* 1987, **181**, L147-L155.
2 P. Liu, J. A. Rodriguez, Y. Takahashi and K. Nakamura, *J. Catal.,* 2009, **262**, 294-303.
3 D. A. King and M. G. Wells, *Surf. Sci.,* 1972, **29**, 454-482.
4 C. Xu and B. E. Koel, *Surf. Sci.,* 1994, **304**, 249-266.
5 J. A. Rodriguez and C. T. Campbell, *J. Catal.,* 1989, **115**, 500-520.
6 J. Gascon, C. Tellez, J. Herguido and M. Menendez, *Appl. Catal. A-Gen.,* 2003, **248**, 105-116.
7 P. Forzatti and L. Lietti, *Catal. Today,* 1999, **52**, 165-181.